

A Binuclear Gold(I) Complex with Mixed Bridging Diphosphine and Bis(N-Heterocyclic Carbene) Ligands Shows Favorable Thiol Reactivity and Inhibits Tumor Growth and Angiogenesis In Vivo**

Taotao Zou, Ching Tung Lum, Chun-Nam Lok, Wai-Pong To, Kam-Hung Low, and Chi-Ming Che*

Abstract: In the design of anticancer gold(I) complexes with high in vivo efficacy, tuning the thiol reactivity to achieve stability towards blood thiols yet maintaining the thiol reactivity to target cellular thioredoxin reductase (TrxR) is of pivotal importance. Herein we describe a dinuclear gold(I) complex (**1**-PF₆) utilizing a bridging bis(N-heterocyclic carbene) ligand to attain thiol stability and a diphosphine ligand to keep appropriate thiol reactivity. Complex **1**-PF₆ displays a favorable stability that allows it to inhibit TrxR activity without being attacked by blood thiols. In vivo studies reveal that **1**-PF₆ significantly inhibits tumor growth in mice bearing HeLa xenograft and mice bearing highly aggressive mouse B16-F10 melanoma. It inhibits angiogenesis in tumor models and inhibits sphere formation of cancer stem cells in vitro. Toxicology studies indicate that **1**-PF₆ does not show systemic anaphylaxis on guinea pigs and localized irritation on rabbits.

By virtue of being strong σ donors to allow formation of stable M–C bond(s), stable N-heterocyclic carbenes (NHCs) have a profound impact in diverse areas of chemistry.^[1] Less developed but with burgeoning interests in recent years is the application of metal NHC complexes in anticancer treatments.^[1a-c,2] The side effects and/or lack of in vivo efficacy of many reported anticancer metal complexes including the classical platinum anticancer drugs can be related to their instability under physiological conditions.^[3] NHC ligand(s) stabilize metal ions against precipitation into metal aggregates under physiological conditions and at the same time can

serve to deliver bioactive metal ions to the cellular target(-s).^[2a,c-g] In fact, there are reports showing that metal complexes containing NHC ligands display potent anticancer properties and are potential drug candidates for drug resistant cancers and have mechanisms of action different from that of cisplatin.^[2a,c-h]

Gold(I) complexes are anticancer active.^[4] Mirabelli, Sadler, and co-workers first reported the apparently thiol-unreactive [Au^I(dppe)₂]⁺ (dppe = 1,2-bis(diphenylphosphanyl)ethane) to display efficacy towards several solid tumor models,^[5] but toxicity was observed in in vivo studies with large animals.^[6] Later studies revealed that the SH/SeH-containing thioredoxin reductase (TrxR) is a potential cellular target of the Au^I ion, and the Au^I ion is able to block the C-terminal -Cys-Sec- site of TrxR through covalent binding with selenol and/or thiol.^[4a,c-p] TrxR inhibition requires a facile ligand-exchange reaction with thiols, but the high thiol affinity of Au^I may lead to covalent binding interactions with blood thiols including albumin and blood glutathione (GSH), resulting in limited bioavailability to tumor tissues.^[4k,n,7] Despite a large number of gold(I) complexes (mostly the mononuclear ones) reported to display TrxR inhibition as well as anti-proliferative properties, examples of Au^I complexes which display in vivo solid tumor inhibition activity are rare.^[8] Thus tuning the thiol reactivity to minimize off-target binding in blood while maintaining enough reactivity to inhibit cellular TrxR could be a guiding principle in the design of new anticancer gold(I) complexes.

Au^I–Au^I interactions can be used to stabilize Au^I ions for medicinal applications. The dinuclear gold(I) complex, [(Ph₃PAu)₂(μ -DTE)] (H₂DTE = 1,4-dimercaptobutane-2,3-diol), could increase the life span of mice bearing Ehrlich-Ascites tumors despite its severe toxicity.^[9] Several dinuclear gold(I) complexes containing bridging bidentate NHC ligands, [Au₂(bis(NHC))₂]²⁺, are not reactive towards thiols and could be used as biological probes.^[10] It was reported that replacing one NHC of the mononuclear [Au^I(NHC)₂]⁺ complexes with PPh₃ would lead to stronger TrxR inhibition.^[11] Herein is described a novel binuclear gold(I) complex (**1**-PF₆, Figure 1) containing mixed diphosphine and bis(NHC) bridging ligands. This complex shows favorable stability in the presence of thiols at blood concentrations, potently inhibits TrxR through a tight-binding mode, and effectively inhibits tumor growth in two independent animal models. This is the first gold(I) complex reported to inhibit cancer stem cell activity and to inhibit in vivo angiogenesis in a tumor model.

[*] T. Zou, Dr. C. T. Lum, Dr. C.-N. Lok, Dr. W.-P. To, Dr. K.-H. Low, Prof. Dr. C.-M. Che
State Key Laboratory of Synthetic Chemistry
Institute of Functional Materials and Department of Chemistry
The University of Hong Kong
Pokfulam Road, Hong Kong (China)
E-mail: cmche@hku.hk
Prof. Dr. C.-M. Che
HKU Shenzhen Institute of Research and Innovation
Shenzhen 518053 (China)

[**] This work was supported by the Innovation and Technology Fund (ITF-Tier 2, ITS/134/09FP) administered by the Innovation and Technology Commission, HKSAR, the National Key Basic Research Program of China (2013CB834802), and the University Grants Committee (Area of Excellence Scheme AoE/P-03/08, HKSAR, China). We thank Dr. Eva Yi-Man Fung and Dr. Kwan-Ming Ng for help in MS analysis.



Supporting information for this article is available on the WWW under <http://dx.doi.org/10.1002/anie.201400142>.

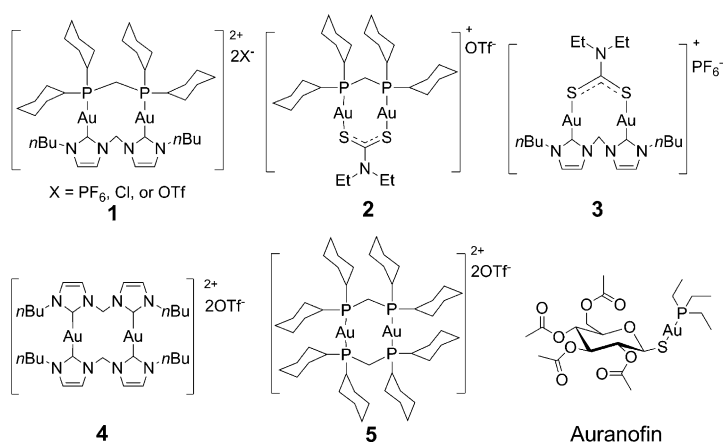


Figure 1. Chemical structures of 1–5 and auranofin. Note that though termed 1-PF₆, the complex is a dication with two PF₆ counterions.

The binuclear gold(I) diphosphine/bis(NHC) complex (**1**) was synthesized by the reaction of [Au₂bis(NHC)Cl₂] and dcpm [dcpm = bis(dicyclohexylphosphine)methane] to give the dicationic species termed **1**-Cl, ion exchange with NH₄PF₆ or LiOTf gave **1**-PF₆ and **1**-OTf (see the Supporting Information). Complexes **2**–**5** (Figure 1) and auranofin were prepared/used for comparative study. The crystal structure of **1**-PF₆ (Figure S1 and Table S1 in the Supporting Information)^[12] shows that the Au...Au distance is 3.083 Å, being slightly longer than that of **5** (2.926–3.013 Å)^[13] but 0.46 Å shorter than that of [Au₂(NHC-C₁-NHC)₂]²⁺ (3.5425 Å).^[14]

The stability of **1**–**5** and auranofin towards bovine serum albumin (BSA) was examined by inductively coupled plasma mass spectrometry (ICP-MS) analysis of the content of unbound (non-covalent) gold in the supernatant obtained from acetone precipitation of the albumin. For **4**, more than 90% of gold was left unbound after incubation of the complex with BSA for 5 h. For **2**, **3**, **5**, or auranofin, less than 30% of unbound gold was observed in each case. In the case of **1**-PF₆, more than 70% free-gold content was observed for the same incubation condition (Figure S2).

Electrospray ionization quadrupole time-of-flight mass spectrometry (ESI-QTOF-MS) was used to investigate the reaction of **1**-PF₆ and GSH. Mixtures of 3 × 10⁻⁶ M of **1**-PF₆ or auranofin (both had a linear response of MS intensity versus concentrations, Figure S3) with 5-fold excess of GSH (1.5 × 10⁻⁵ M) at pH 8.0 were freshly prepared and the ion intensity of the gold complex was recorded (Figure 2). After mixing with GSH, there was a rapid decrease in the ion intensity of

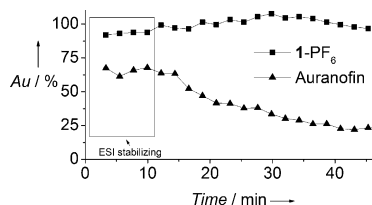


Figure 2. The residual gold complex after mixing **1**-PF₆ (■) or auranofin (▲) and GSH as determined by ESI-QTOF-MS. The amount of residual gold(I) complex was determined as the percentage of initial ion intensity recorded before GSH addition.

auranofin (*m/z* 679.1) with 20% remaining after 45 min. An intermediate with *m/z* value consistent with glutathione-gold-phosphine adduct GS-Au-PET₃ (*m/z* 622.1) appeared initially followed by gradual decrease of its ion intensity (Figure S4). On the contrary, no significant change of the ion intensity of **1**²⁺ (*m/z* 531.2) was found during the first 45 min of incubation with GSH, indicating that **1**-PF₆ was not reactive towards GSH at this concentration. When a higher concentration of GSH (5 × 10⁻⁵ M) was used, the ion intensity of auranofin decreased with a faster rate while that of **1**²⁺ was retained at approximate the initial level (Figure S5). As GSH (1–10 μM) and serum albumin (35–50 mg mL⁻¹) are the major thiol-containing compounds present in blood,^[15] the binuclear gold(I) complex **1**-PF₆ appears to be moderately stable towards blood thiols.

The interaction of **1**-PF₆ with GSH was further studied by ESI-QTOF-MS analysis upon further increasing the concentrations of **1**-PF₆ and GSH. When 1.5 × 10⁻⁴ M of **1**-PF₆ was incubated with excess GSH (5 × 10⁻⁴ M) for 1 h, small but distinct peaks at *m/z* 764.3 (*z* = +1), 684.8 (*z* = +2), and 605.3 (*z* = +2) appeared, which are attributed to [Au(NHC-Im)(GS)]⁺, [Au₂(dcpm)(NHC-Im)(GS)]²⁺ (Im = imidazolium), and [Au₂(dcpm)₂]²⁺, respectively (Figure S6).

We examined the effect of serum albumin on the cytotoxicity of the gold(I) complexes. After pre-incubation of these gold(I) complexes in minimal essential medium (MEM) with/without BSA (40 mg mL⁻¹) for 1 h, and then adding the resulting media into HeLa cells for further 24 h incubation, the cell viability was determined by MTT assays. As shown in Table 1, BSA can significantly suppress the

Table 1. Cytotoxic IC₅₀ (μM) of the gold(I) complexes incubated in BSA-free and BSA-containing media for 24 h as determined by MTT assays.

	1-PF ₆	2	3	4	5	Auranofin
BSA-free	13.5	3.1	1.5	46.5	0.8	1.1
BSA	46.1	16.5	7.34	> 300	17.9	49.3
ratio ^[a]	0.293	0.187	0.198	< 0.09	0.042	0.023

[a] Ratios were calculated by the IC₅₀ of BSA-free divided by the IC₅₀ of the BSA-containing condition. All the IC₅₀ values were determined from at least three independent experiments.

cytotoxicity of the gold(I) complexes. The cytotoxicity of **1**-PF₆ was less affected compared to the other more thiol-reactive **2**, **3**, **5** and auranofin. The relatively thiol-unreactive complex **4** is less cytotoxic in both BSA-containing and BSA-free media. Although **4** is inert towards thiols, serum albumin has a big impact on its cytotoxicity; the presence of BSA was observed to render **4** to be almost non-toxic (IC₅₀ > 300 μM).

Complex **1**-PF₆ is also cytotoxic towards breast adenocarcinoma (MCF-7), nasopharyngeal carcinoma (SUNE1), lung adenocarcinoma (H1975), and mouse melanoma (B16-F10) with IC₅₀ values ranging from 1.3 ± 0.2 to 3.2 ± 1.0 μM; these IC₅₀ values are up to 13.5-fold greater than those of cisplatin (Table S2). Complexes **1**-Cl and **1**-OTf showed cytotoxicity similar to that of **1**-PF₆ in in vitro cytotoxicity studies.

The inhibitory effect of **1**-PF₆ on purified TrxR was studied. Treatment of recombinant rat TrxR1 (2 nM) with 200 nM of **1**-PF₆ in the presence of NADPH resulted in a time-dependent reduction of TrxR activity by over 90% in 2 h (Figure S7). In addition, complex **1**-PF₆ inhibited TrxR more potently than the structurally related glutathione reductase (GR), with the IC₅₀ values being 38 nM and 10 μM respectively, using DTNB as the substrate (Figure S8,9). The TrxR inhibition mechanism was studied by progressive curve analysis^[8d,16] of the time course of TrxR inhibition. The progress curves are non-linear (Figure 3 a), revealing a two-phase equilibrium that is typical of slow-onset tight-binding mode of inhibition. Plotting the observed first-order rate constants, k_{app} , against the concentration of **1**-PF₆ gave a hyperbolic function curve (Figure 3 b), indicating a two-step binding mechanism, where the initial collision complex (EI) is rapidly formed followed by a subsequent isomerization that enhances the tightness of enzyme-inhibitor complex (EI*, Figure 3 b inset). Fitting the time course data gave the values of $k_3 = 0.0260 \text{ s}^{-1}$, $k_4 = 0.0020 \text{ s}^{-1}$, $K_1 = 413 \text{ nM}$, $K_1^* = 28.5 \text{ nM}$. Meanwhile, in the presence of 2 mM GSH, the inhibitory activities on NADPH-TrxR-Trx-insulin system by **1**-PF₆ were not attenuated but rather moderately enhanced with IC₅₀ decreased from 5.56 μM to 3.29 μM, but the inhibition by auranofin under the same conditions decreased (Figure S10).

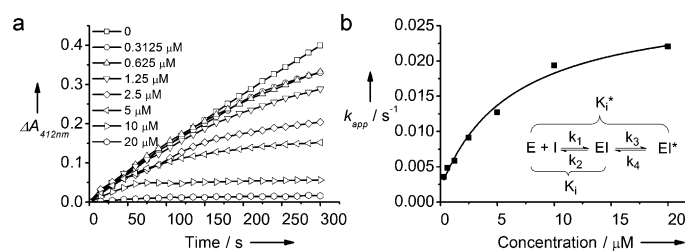


Figure 3. a) Time dependence to the onset of TrxR inhibition by **1**-PF₆. b) Plot of k_{app} (determined by fitting the data in Figure 3 a) against concentrations of **1**-PF₆ suggests a two-step binding mechanism. Inset: two-step inhibition mechanism.

Several peptides have been used in the study of the binding mode of gold(I) with the active site of TrxR.^[4j,n,17] In this work, the C-terminal GCUG motif (Gly-Cys-Sec-Gly) was used as the model (Figure 4). Incubation of 0.5 mM of **1**-PF₆ with GCUG at the same concentration in 5 mM NH₄HCO₃ with 50% MeOH (v/v) for 1 h, 4 h, and 24 h resulted in all cases formation of a new species with m/z 1187.2500 (Figure S11a). Both the m/z value and isotope pattern of this new species match the formulation of tetrapeptide with a bound [Au₂dcpm]²⁺ having calculated m/z 1187.2488 (Figure S11b, error: 1.0 ppm). Meanwhile, the ¹H NMR signals at 6.0–8.0 ppm are indicative of the release of bis(NHC) ligand (Figure 4b) and the ¹H signals of β-CH₂ of Cys and Sec are also significantly shifted, further indicating coordination of S and Se atoms to Au atom/ion. Notably, two [AuPEt₃]⁺ units of auranofin were reported to bind to both SeH and SH of the

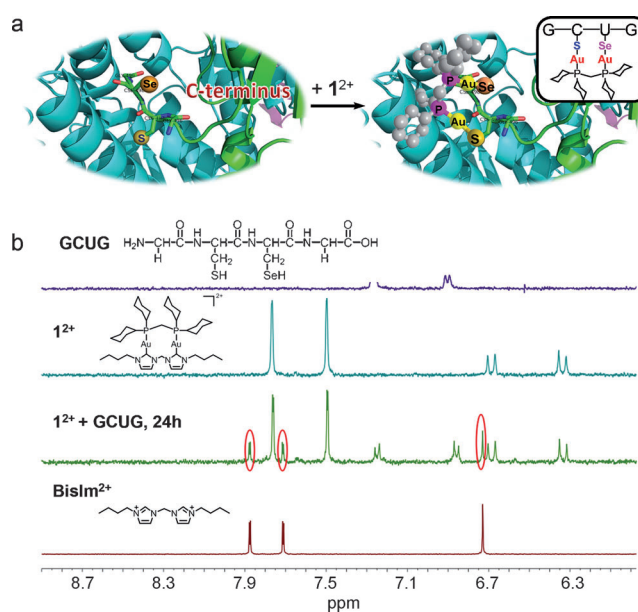


Figure 4. a) Proposed binding interaction of **1**-PF₆ with TrxR. Inset: binding mode based on MS results. b) ¹H NMR spectra (400 MHz) of GCUG (top), **1**-PF₆ (upper middle), equal molar of **1**-PF₆ with GCUG (lower middle) and [bis(Im)]²⁺ ligand (bottom) in D₂O/[D₆]DMSO = 1:1 (v/v, phosphate buffer, pH* = 7.4) after 24 h incubation.

GCUG motif.^[17a] In the present case, **1**-PF₆ is bound to GCUG motif in 1:1 molar ratio through simultaneous coordination of the binuclear Au^I unit to respective S and Se of the contiguous Cys and Sec residues, accompanied by the release of bis(NHC) but not dcpm ligand.

Cancer stem cells (CSCs) having the ability of self-renewal and differentiation have been proposed to cause relapse and metastasis by giving rise to new tumors.^[18] The ability to form spheres in non-adherent cultures is a characteristic of CSCs. Herein we employed sphere-formation assay to examine the effect of **1**-PF₆ on the population of HeLa cells. As shown in Figure 5, free-floating spheres were observed in the solvent-control group, and treatment of HeLa cells with 5 or 10 μM of **1**-

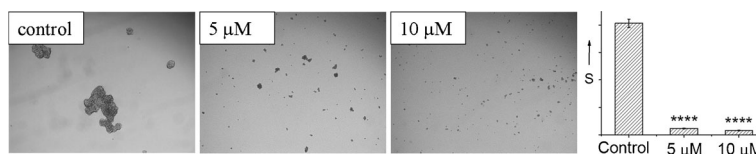


Figure 5. Inhibition of sphere formation of HeLa cells by **1**-PF₆. Left: representative pictures from three independent experiments. Right: relative area (s) occupied by spheres per microscopic field. Data are shown as mean from three independent experiments. **** $p < 0.0001$ compared to solvent control.

PF₆ resulted in statistically significant inhibition ($p < 0.0001$) of the self-renewal (sphere-forming) ability. Similar results were found in U-87 MG human glioblastoma cells (Figure S12). These data revealed that **1**-PF₆ could inhibit the self-renewal ability of CSCs.

As complexes **1**–**5** are insoluble in water, biocompatible PET (60% polyethylene glycol 400; 30% ethanol; 10%

Tween-80) was used as excipient for in vivo study. The complexes were dissolved in PET which was diluted with PBS (final PET: 1.5–4%, v/v). Complexes **1-Cl** and **1-OTf** could be dissolved in the buffer to give a clear solution. Complex **1-PF₆** gave a finely dispersed suspension that remained stable for several hours. Light scattering experiment indicated the formation of nanoparticles (diameter size of 175 ± 81 nm). TEM analysis revealed that the particles formed from **1-PF₆** were well dispersed with diameters of 144 ± 50 nm (Figure S13). Complexes **2**, **3**, and **5** were observed to form similar suspensions.

The in vivo antitumor effect of the gold(I) complexes was examined. After treatment of nude mice bearing HeLa xenografts with 5 mg kg^{-1} of **1-PF₆** through intraperitoneal (i.p.) injection once every three days, significant tumor volume inhibition by 79% ($p < 0.05$) and 81% ($p < 0.05$) was found compared to those treated with solvent control after 6 and 9 days of treatment, respectively (Figure 6). In addition, no mouse death or body weight loss was observed

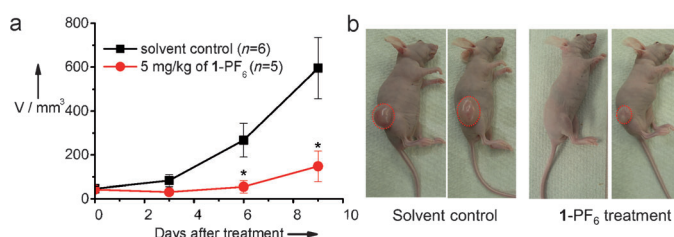


Figure 6. Antitumor effect of **1-PF₆** on mice bearing HeLa xenografts. a) Changes of tumor volume (V) after treatment with **1-PF₆**; * $p < 0.05$. b) Representative mouse photos after 9 days of treatment.

after the treatment with **1-PF₆** at this dosage (Figure S14). We further tested the inhibition effects towards the highly aggressive, poorly immunogenic mouse melanoma (B16-F10) model in C57BL/6N mice. As shown in Figure S15a, while the tumor in solvent control group grew at least three times faster than HeLa xenograft, significant tumor inhibition (62%, $p < 0.05$) could be achieved after administration (i.p.) with 15 mg kg^{-1} of **1-PF₆** once every 2–3 days for 8 days. The treatment also did not cause mouse death or body weight loss (Figure S15b).

Complexes **1-Cl** and **1-OTf** could also inhibit tumor growth of mice bearing HeLa xenografts at a higher treatment frequency. After administration of **1-Cl** or **1-OTf** at dosage of 5 mg kg^{-1} every day, statistically significant difference could be obtained compared to solvent control, with final tumor growth inhibition of 47.7% ($p < 0.01$) and 35.1% ($p < 0.05$), respectively (Figure S16). Again, no mouse death or mouse body weight loss was found. These findings revealed that both the gold complex cation and counteranion can significantly affect the in vivo antitumor effect. Presumably the anion affects the solubility and hence pharmacokinetics of complex **1** salt in the blood serum. A recent report showed that the formation of nanoparticles through the incorporation of appropriate anions could increase the anticancer properties.^[19] Formation of nanoparticles could be beneficial in the present case. This factor, however, is not sufficient alone to

achieve in vivo antitumor efficacy, as the highly thiol-reactive complexes **2**, **3**, and **5**, all of which could also form nanoparticles, did not exhibit inhibition of HeLa xenografts (Figure S17).

In another treatment, a rather low dosage, 0.6 mg kg^{-1} , of **1-PF₆** was used to treat mice bearing a HeLa xenograft (i.p. injection); statistically significant tumor growth inhibition was obtained after 6 days of treatment, with final inhibition of 59.3% after 14 days of treatment (Figure S18). Collectively, the therapeutic window of **1-PF₆** could be quite large since 0.6 mg kg^{-1} to 15 mg kg^{-1} all resulted in significant antitumor effects.

The in vivo anti-angiogenic effect of gold(I) complexes has been reported by Ott and co-workers using zebrafish model.^[4n,20] In our study, the anti-angiogenic effect of **1-PF₆** was examined by immune-histochemical detection of the CD31 (cluster of differentiation 31) of the blood microvessels in the tumor tissue of mice bearing HeLa xenografts (5 mg kg^{-1}). The average number of microvessels per microscopic field of **1-PF₆**-treated tumor was 2.35 (Figure 7), while that treated with solvent control was 4.34 ($p < 0.05$), indicating that **1-PF₆** could significantly inhibit angiogenesis of HeLa xenografts (Figure S19).

To examine the side effects, we have conducted toxicology studies of **1-PF₆** in a State Food and Drug Administration, P. R. China (SFDA)-approved laboratory (Tianjin Institute of Pharmaceutical Research). All system anaphylaxis reaction was tested in guinea pigs. The animals were treated with 0.9% saline injection (negative control), 10% PET solvent, 1% ovalbumin in saline (positive control) and 0.12 mg kg^{-1} of **1-PF₆** in PET solvent, respectively, through i.p. injection every other day for a total of

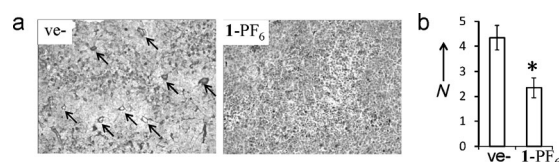


Figure 7. a) Immunohistochemical detection of CD31 in the tumor tissues. Arrows indicate CD31 microvessels. b) Average number (N) of microvessels per microscopic field. * $p < 0.05$, compared to solvent control.

5 times; after 14 days, forelimbs of guinea pigs were injected intravenously (i.v.) with 2-fold dosage. All guinea pigs in the positive control group exhibited severe allergic reaction (eventually died), but **1-PF₆** treatment group did not show allergic reaction. The blood-vessel irritation test was also performed. Complex **1-PF₆** (0.12 mg) was directly injected into the auricular veins of the rabbits, and the histopathology was examined after 4 days and 14 days of treatment. No apparent ear blood vessel dilatation, bleeding, swelling, or other morphological changes were found at the administration sites upon treatment with **1-PF₆**. (See details in Supporting Information). These results revealed that **1-PF₆** did not show systemic anaphylaxis and localized irritation.

In summary, the binuclear gold(I) complex **1-PF₆** shows favorable thiol reactivity and meanwhile is a tight-binding

inhibitor of TrxR. This complex significantly inhibited tumor growth of HeLa xenografts and highly aggressive mouse B16-F10 melanoma with no observable side effects under in vivo conditions. This finding sheds lights on the clinical prospects of developing gold(I)-NHC complexes into useful anticancer drugs. Future works will focus on investigating the binding interactions of this dinuclear gold(I) complex with other thiol-containing enzymes/proteins and eliciting the anticancer mechanism(s) of action through proteomics and transcriptomics studies.

Received: January 7, 2014

Published online: April 11, 2014

Keywords: antitumor agents · gold(I) · N-heterocyclic carbenes · thiol reactivity · thioredoxin reductase (TrxR)

- [1] a) H. G. Raubenheimer, S. Cronje, *Chem. Soc. Rev.* **2008**, *37*, 1998–2011; b) J. C. Y. Lin, R. T. W. Huang, C. S. Lee, A. Bhattacharyya, W. S. Hwang, I. J. B. Lin, *Chem. Rev.* **2009**, *109*, 3561–3598; c) L. Merce, M. Albrecht, *Chem. Soc. Rev.* **2010**, *39*, 1903–1912; d) M. Melaimi, M. Soleilhavoup, G. Bertrand, *Angew. Chem.* **2010**, *122*, 8992–9032; *Angew. Chem. Int. Ed.* **2010**, *49*, 8810–8849; e) D. Martin, M. Soleilhavoup, G. Bertrand, *Chem. Sci.* **2011**, *2*, 389–399; f) S. P. Nolan, *Acc. Chem. Res.* **2011**, *44*, 91–100; g) H. D. Velazquez, F. Verpoort, *Chem. Soc. Rev.* **2012**, *41*, 7032–7060; h) J. Izquierdo, G. E. Hutson, D. T. Cohen, K. A. Scheidt, *Angew. Chem.* **2012**, *124*, 11854–11866; *Angew. Chem. Int. Ed.* **2012**, *51*, 11686–11698; i) S. Gaillard, C. S. J. Cazin, S. P. Nolan, *Acc. Chem. Res.* **2012**, *45*, 778–787; j) A. Grossmann, D. Enders, *Angew. Chem.* **2012**, *124*, 320–332; *Angew. Chem. Int. Ed.* **2012**, *51*, 314–325; k) M. Fèvre, J. Pinaud, Y. Gnanou, J. Vignolle, D. Taton, *Chem. Soc. Rev.* **2013**, *42*, 2142–2172.
- [2] a) K. M. Hindi, M. J. Panzner, C. A. Tessier, C. L. Cannon, W. J. Youns, *Chem. Rev.* **2009**, *109*, 3859–3884; b) A. John, P. Ghosh, *Dalton Trans.* **2010**, *39*, 7183–7206; c) J. J. Yan, A. L.-F. Chow, C.-H. Leung, R. W.-Y. Sun, D.-L. Ma, C.-M. Che, *Chem. Commun.* **2010**, *46*, 3893–3895; d) R. W.-Y. Sun, A. L.-F. Chow, X.-H. Li, J. J. Yan, S. S.-Y. Chui, C.-M. Che, *Chem. Sci.* **2011**, *2*, 728–736; e) L. Oehninger, R. Rubbiani, I. Ott, *Dalton Trans.* **2013**, *42*, 3269–3284; f) F. Cisnetti, A. Gautier, *Angew. Chem.* **2013**, *125*, 12194–12196; *Angew. Chem. Int. Ed.* **2013**, *52*, 11976–11978; g) W. Liu, R. Gust, *Chem. Soc. Rev.* **2013**, *42*, 755–773; h) T. Zou, C.-N. Lok, Y. M. E. Fung, C.-M. Che, *Chem. Commun.* **2013**, *49*, 5423–5425.
- [3] P. J. Sadler, C. Muncie, M. Shipman in *Biological Inorganic Chemistry: Structure and Reactivity* (Eds.: I. Bertini, H. B. Gray, E. I. Stiefel, J. S. Valentine), University Science Books, New York, **2006**, pp. 95–135.
- [4] a) S. Urig, K. Fritz-Wolf, R. Réau, C. Herold-Mende, K. Tóth, E. Davioud-Charvet, K. Becker, *Angew. Chem.* **2006**, *118*, 1915–1920; *Angew. Chem. Int. Ed.* **2006**, *45*, 1881–1886; b) S. Ray, R. Mohan, J. K. Singh, M. K. Samantaray, M. M. Shaikh, D. Panda, P. Ghosh, *J. Am. Chem. Soc.* **2007**, *129*, 15042–15053; c) J. L. Hickey, R. A. Ruhayel, P. J. Barnard, M. V. Baker, S. J. Berners-Price, A. Filipovska, *J. Am. Chem. Soc.* **2008**, *130*, 12570–12571; d) A. Bindoli, M. P. Rigobello, G. Scutari, C. Gabbiani, A. Casini, L. Messori, *Coord. Chem. Rev.* **2009**, *253*, 1692–1707; e) I. Ott, *Coord. Chem. Rev.* **2009**, *253*, 1670–1681; f) E. Meggers, *Chem. Commun.* **2009**, 1001–1010; g) S. Nobili, E. Mini, I. Landini, C. Gabbiani, A. Casini, L. Messori, *Med. Res. Rev.* **2010**, *30*, 550–580; h) C.-M. Che, F.-M. Siu, *Curr. Opin. Chem. Biol.* **2010**, *14*, 255–261; i) G. Gasser, I. Ott, N. Metzler-Nolte, *J. Med. Chem.* **2011**, *54*, 3–25; j) K. P. Bhabak, B. J. Bhuyan, G. Mughesh, *Dalton Trans.* **2011**, *40*, 2099–2111; k) S. J. Berners-Price, A. Filipovska, *Metallomics* **2011**, *3*, 863–873; l) C.-M. Che, R. W.-Y. Sun, *Chem. Commun.* **2011**, *47*, 9554–9560; m) A. Casini, L. Messori, *Curr. Top. Med. Chem.* **2011**, *11*, 2647–2660; n) A. Meyer, C. P. Bagowski, M. Kokoschka, M. Stefanopoulou, H. Alborzina, S. Can, D. H. Vlecken, W. S. Sheldrick, S. Wölfl, I. Ott, *Angew. Chem.* **2012**, *124*, 9025–9030; *Angew. Chem. Int. Ed.* **2012**, *51*, 8895–8899; o) I. Romero-Canelón, P. J. Sadler, *Inorg. Chem.* **2013**, *52*, 12276–12291; p) T. Zou, C. T. Lum, S. S.-Y. Chui, C.-M. Che, *Angew. Chem.* **2013**, *125*, 3002–3005; *Angew. Chem. Int. Ed.* **2013**, *52*, 2930–2933.
- [5] S. J. Berners-Price, C. K. Mirabelli, R. K. Johnson, M. R. Mattern, F. L. McCabe, L. F. Faucette, C.-M. Sung, S.-M. Mong, P. J. Sadler, S. T. Crooke, *Cancer Res.* **1986**, *46*, 5486–5493.
- [6] a) G. D. Hoke, R. A. Macia, P. C. Meunier, P. J. Bugelski, C. K. Mirabelli, G. F. Rush, W. D. Matthews, *Toxicol. Appl. Pharmacol.* **1989**, *100*, 293–306; b) P. F. Smith, G. D. Hoke, D. W. Alberts, P. J. Bugelski, S. Lupo, C. K. Mirabelli, G. F. Rush, *J. Pharmacol. Exp. Ther.* **1989**, *249*, 944–950.
- [7] a) N. A. Malik, G. Otiko, P. J. Sadler, *J. Inorg. Biochem.* **1980**, *12*, 317–322; b) S. J. Berners-Price in *Bioinorganic Medical Chemistry*, Wiley-VCH, Weinheim, **2011**, pp. 197–222.
- [8] a) N. Pillarsetty, K. K. Katti, T. J. Hoffman, W. A. Volkert, K. V. Katti, H. Kamei, T. Koide, *J. Med. Chem.* **2003**, *46*, 1130–1132; b) M. Stallings-Mann, L. Jamieson, R. P. Regala, C. Weems, N. R. Murray, A. P. Fields, *Cancer Res.* **2006**, *66*, 1767–1774; c) C. H. Chui, R. S.-M. Wong, R. Gambari, G. Y.-M. Cheng, M. C.-W. Yuen, K.-W. Chan, S.-W. Tong, F.-Y. Lau, P. B.-S. Lai, K.-H. Lam, C.-L. Ho, C.-W. Kan, K. S.-Y. Leung, W.-Y. Wong, *Bioorg. Med. Chem.* **2009**, *17*, 7872–7877; d) K. Yan, C.-N. Lok, K. Bierla, C.-M. Che, *Chem. Commun.* **2010**, *46*, 7691–7693.
- [9] C. F. Shaw III, A. Beery, *Inorg. Chim. Acta* **1986**, *123*, 213–216.
- [10] P. J. Barnard, L. E. Wedlock, M. V. Baker, S. J. Berners-Price, D. A. Joyce, B. W. Skelton, J. H. Steer, *Angew. Chem.* **2006**, *118*, 6112–6116; *Angew. Chem. Int. Ed.* **2006**, *45*, 5966–5970.
- [11] R. Rubbiani, S. Can, I. Kitanovic, H. Alborzina, M. Stefanopoulou, M. Kokoschka, S. Mönchgesang, W. S. Sheldrick, S. Wölfl, I. Ott, *J. Med. Chem.* **2011**, *54*, 8646–8657.
- [12] CCDC 979735 contains the supplementary crystallographic data for this paper. These data can be obtained free of charge from The Cambridge Crystallographic Data Centre via www.ccdc.cam.ac.uk/data_request/cif.
- [13] W.-F. Fu, K.-C. Chan, V. M. Miskowski, C.-M. Che, *Angew. Chem.* **1999**, *111*, 2953–2955; *Angew. Chem. Int. Ed.* **1999**, *38*, 2783–2785.
- [14] P. J. Barnard, M. V. Baker, S. J. Berners-Price, B. W. Skelton, A. H. White, *Dalton Trans.* **2004**, 1038–1047.
- [15] S. Santra, C. Kaittanis, O. J. Santiesteban, J. M. Perez, *J. Am. Chem. Soc.* **2011**, *133*, 16680–16688.
- [16] a) V. Vathipadiekal, M. Rao, *J. Biol. Chem.* **2004**, *279*, 47024–47033; b) C. Xu, R. Hall, J. Cummings, F. M. Raushel, *J. Am. Chem. Soc.* **2006**, *128*, 4244–4245.
- [17] a) A. Pratesi, C. Gabbiani, M. Ginanneschi, L. Messori, *Chem. Commun.* **2010**, *46*, 7001–7003; b) J. Lee, L. P. Jayathilaka, S. Gupta, J. S. Huang, B. S. Lee, *J. Am. Soc. Mass Spectrom.* **2012**, *23*, 942–951.
- [18] M. Dean, T. Fojo, S. Bates, *Nat. Rev. Cancer* **2005**, *5*, 275–284.
- [19] P. K. S. Magut, S. Das, V. E. Fernandez, J. Losso, K. McDonough, B. M. Naylor, S. Aggarwal, I. M. Warner, *J. Am. Chem. Soc.* **2013**, *135*, 15873–15879.
- [20] I. Ott, X. Qian, Y. Xu, D. H. W. Vlecken, I. J. Marques, D. Kubutat, J. Will, W. S. Sheldrick, P. Jesse, A. Prokop, C. P. Bagowski, *J. Med. Chem.* **2009**, *52*, 763–770.